

# The F+HD Reaction: Cross Sections and Rate Constants on an *ab initio* Potential Energy Surface

F. J. Aoiz<sup>a</sup>, L. Bañares<sup>a</sup>, V. J. Herrero<sup>b</sup>, V. Sáez Rábanos<sup>c</sup>, K. Stark<sup>d</sup>, I. Tanarro<sup>b</sup>,  
H.-J. Werner<sup>d</sup>,

a) Departamento de Química Física, Facultad de Química, Universidad Complutense,  
28040 Madrid, Spain.

b) Instituto de Estructura de la Materia (CSIC). Serrano 123, 28006 Madrid Spain.

c) Departamento de Química General y Bioquímica, ETS Ingenieros de Montes,  
Universidad Politécnica, 28040 Madrid. Spain.

d) Institut für Theoretische Chemie, Universität Stuttgart, Pfaffenwaldring 55,  
D-70569 Stuttgart, Germany.

## Abstract

Reaction cross sections and rate constants for the  $F+HD$  reaction have been calculated on the recently released Stark-Werner (SW) *ab initio* potential energy surface (PES) using the quasiclassical trajectory (QCT) method. The results are compared to other theoretical calculations on different PESs and to experimental isotopic branching ratios. The general agreement is good. Dynamical features related to the asymmetric nature of the HD molecule are also discussed.

## 1. Introduction

From a dynamical point of view, the  $F+HD$  reaction is the most interesting isotopic variant of the prototypic  $F+H_2$  system due to the fact that the fluorine atom can attack either of the two ends of the  $HD$  molecule, thus leading to a sampling of different regions of the potential energy surface (PES). The different reactivity of the two exit channels has been a subject of experimental study since the early kinetic investigations of Kompa et al. [1], Persky [2], and Berry [3]. Later works based on two laser schemes [4,5] and, in particular, the celebrated molecular beam experiment of Lee and co-workers [6], have added more detailed information about the distinct dynamical properties of the two channels of the system.

The effect of the mass asymmetry on the dynamics of this reaction has been assessed in a number of theoretical works over the last twenty years. Up to now the majority of these studies (see refs. [5,7] and references cited therein) has been carried out using potential energy surfaces with collinear barriers and relatively narrow bending potentials like the Muckermann 5 (M5) PES [8]. However, in the last years numerous theoretical investigations [9-12] indicated a non collinear transition state with a very flat bending potential. As a consequence, most of the previous theoretical calculations, although interesting for the elucidation of general dynamical effects in reactions of the  $A+BC$  type, do not provide reliable information about the reactivity of the actual  $F+HD$  system.

A fully *ab initio* PES for the  $F+H_2$  reaction has recently been constructed by Stark and Werner [12] (hereafter SW-PES). The comparison between dynamical calculations performed on this PES and experimental data indicates that this surface is the most accurate one to date (see the references cited in [12]). With this PES, QCT calculations for the  $F+HD$  system at low collision energies ( $E_T$ ) have been carried out [13]. This investigation showed that the experimental angular and velocity distributions of the  $DF$  product [6] can be reproduced successfully. However, significant discrepancies were found in the  $HF$  reaction channel. Although for this isotopic variant no quantum

mechanical (QM) calculations have been reported yet, a recent QM work by Castillo et al. [14] on differential cross sections for  $F+H_2$  strongly suggests that the discrepancies for the  $HF$  channel found in the classical results are most likely due to tunneling.

Besides the dynamical studies commented on in the previous paragraph, the available data from macroscopic kinetics are also very valuable for the assessment of the PES; in particular, the absolute value of the thermal rate constant,  $k(T)$ , is at the time the best indication of the reactive size and thus of the correctness of the barrier height. Rosenman and Persky [15] have performed a QCT study of rate constants and branching ratios for the  $F+H_2/F+D_2$ , and  $F+HD$  reaction on the T5 [16,17] and 6SEC [11] PESs. The results from the more realistic 6SEC-PES were found to be in much better accordance with experiment than those from the collinear T5-PES. Subsequent QM calculations of Rosenman et al. [18] for  $F+H_2$  and  $F+D_2$  on the 6SEC-PES were in very good agreement with the QCT cross sections and thermal rate constants.

In a previous letter [19] we have calculated the rate constants for  $F+H_2$  and  $F+D_2$  using the QCT method on the SW-PES. The agreement with experiment was good and, especially for the  $F+H_2$  isotopic variant, better than that obtained with the 6SEC surface, but the calculated rate constants were still smaller than most experimental values. In a very recent work, Rosenman et al. [20] have used the coupled-states approximation and negative imaginary boundary absorbing potentials for the calculation of QM cross sections and rate constants for  $F+H_2$  and  $F+D_2$  on the SW-PES. Noticeable differences are found between classical and quantal results on this surface. The largest discrepancies correspond to the threshold region, where the coupled-states QM calculations predict a practically zero collision energy threshold for the reaction irrespective of the initial rotational state ( $j$ ) of the reacting molecule; the classical thresholds, albeit small, are always larger than zero and are dependent on  $j$ . This discrepancy between classical and quantal results is in contrast to the behavior observed on the 6SEC surface and indicates that tunneling effects are clearly more important for the SW-PES. As the collision energy increases for  $j>0$ , the agreement between the two sets of calculations becomes much better, especially for  $F+D_2$ . Since the threshold region dominates the  $k(T)$  values at

temperatures below 400K, the QM rate constants are clearly larger than the corresponding classical ones, particularly at low temperatures. In fact, the coupled-states QM rate constants are even larger than the measured values, thus suggesting that a deeper investigation, both experimental and theoretical, of this reactive system would be of interest.

In the present work we have extended the QCT investigation on the SW-PES to the  $F+HD$  reaction and have calculated state selective cross sections and rate constants, as well as thermal rate constants in the range of temperatures of the available measurements. The results are discussed in terms of the properties of the PES. Especial attention is dedicated to the intramolecular branching ratio and, in general, to the peculiar effects of the mass asymmetry on the SW-PES used. The results are also compared to calculations on other surfaces and to experimental data.

## 2. Method

The general method for the calculation of the excitation function  $\sigma_R(E_T)$  (i.e., the collision energy dependence of the reaction cross section) has been described previously [19,21]. For each of the rotational states of the  $HD$  molecule the collision energy of the trajectories was sampled randomly between the threshold for reaction and 0.8 eV. Once the collision energy had been chosen within this interval, the impact parameters were selected randomly between zero and a maximum value obtained as indicated in refs. [19,21].

The assignment of the molecular rotational quantum numbers was done by using the semiclassical quantization scheme as suggested by Azriel et al. [22], in which the square of the rotational angular momentum of the molecule is equated to  $(j+1/2)^2 \hbar^2$ . For the temperature range of the available experimental data, individual rotational states from  $j=0$  till  $j=6$  had to be included. A batch of 60,000 trajectories was run for each rotational state. With this  $j$ -specific excitation functions, state specific rate constants and thermal

rate constants for the two exit channels in the range from 150 to 500 K have been calculated as indicated in Ref. [21].

### 3. Results and discussion

Figure 1 shows the cross sections for the two exit channels of the title reaction. The excitation functions corresponding to the reaction leading to  $HF$  (upper panel) are in strong contrast with those leading to  $DF$  (lower panel). For  $j=0$ , the absolute values of the excitation functions indicate that the  $D$  end of the molecule is favorably attacked by the  $F$  atom. The fact that the center of mass of the  $HD$  molecule is closer to the  $D$  atom implies a greater cone of acceptance for this atom, as pointed out by Johnston et al. [5]. Thus the reaction with this end of the molecule will be more likely. In addition, as shown in a previous investigation [13] on the SW-PES, at low collision energies, trajectories attacking either end of the  $HD$  molecule tend to be oriented towards the opposite side, this tendency being more pronounced for the  $H$  end of the molecule due to the mass asymmetry. This effect is less marked when the collision energy is increased. In this case, the reactivity tends to be equalized in both channels. When the molecule is rotationally excited, the evolution of the  $\sigma_R(E_T, j)$  curves is also very different in each channel. The reactivity at the  $HF$  channel increases considerably with the rotational excitation of the  $HD$  molecule, whereas it decreases in the  $DF$  channel. This is in clear contrast to the behavior obtained on the M5-PES [7] where at low collision energies the reactivity decreases for both channels with growing  $j$ .

The effect of rotation on the SW-PES is twofold: firstly, rotation of the  $HD$  molecule diminishes the orienting influence of the surface [13] to a great extent, leading to an enhancement of the reaction with the  $H$  end. Furthermore, the longer arm of the  $H$  end [5] implies that trajectories are more likely to reach the barrier at this end; in other words, when the  $HD$  molecule rotates about its center of mass, the radius of the sphere spanned by the  $H$  atom is larger and the  $D$  end of the molecule is screened by the  $H$  end. This second effect decreases with growing translational energy and, as shown in Fig 1, the reaction cross section in the  $HF$  channel for  $j>1$  falls or remains constant with

growing  $E_T$ , while in the  $DF$  channel rises slightly. A recrossing mechanism can also contribute to the decrease in the cross section for the formation of  $HF$ . Recrossing will be more likely for collisions of the  $F$  atom with the  $H$  end because the lighter  $H$  atom will leave the triatomic reaction intermediate more rapidly than the  $D$  atom [23], and also due to the fact that, in this case, the repulsive barrier is found at larger distances and this implies more radial energy.

The excitation functions shown in Fig. 1 were used to calculate thermal rate constants for each of the initial rotational states,  $k(T,j)$ , for temperatures up to 500 K; this temperature range essentially samples the post-threshold region of the excitation functions. The values of the state specific rate constants are listed in Table 1 and do not include the ‘multisurface correction factor’ (see for instance Ref. [24] and references therein). For the  $HF$  channel, the initial rotation of the  $HD$  molecule has always a neat beneficial effect on  $k(T,j)$ , which is especially pronounced at low  $T$ . For the  $DF$  exit channel the effect of rotation on  $k(T,j)$  is much less marked.

Thermal rate constants,  $k(T)$ , for the production of  $HF$  and  $DF$  in the  $T$  range between 159 and 500 K are listed in Table 2 and shown in Fig. 2, together with the QCT results of Rosenman and Persky [15] on the 6SEC-PES. The QCT values in Table 2 include the temperature dependent multisurface correction factor, which accounts for the statistical population of the asymptotic  $^2P_{3/2}$  and  $^2P_{1/2}$  states assuming that non-adiabatic transitions can be neglected [24]. Over the whole temperature range studied, and for both exit channels, the  $k(T)$  obtained on the SW-PES are larger than those obtained on the 6SEC one, the differences between the results on the two surfaces are largest ( $\approx 35\text{--}40\%$ ) at the lowest temperature considered (159 K) and decrease to about 10% at 413 K. Although the rate constants for this isotopic variant of the reaction have not been measured directly, ‘recommended values’ can be found in the literature [25]. These values have been estimated from the results of different works using mainly the measured rate constants for  $F+H_2$  and  $F+D_2$  and the experimentally determined ratios of these rate constants to those of  $F+HD$  and  $DH$  (see the references. cited in [25]). The recommended values from Ref. [25] are in better agreement with the QCT results on the

SW-PES than with those on the 6SEC-PES. At 298 K, for instance, the rate constants of the reference [25] are  $1 \times 10^{-11}$  and  $7.2 \times 10^{-12}$   $\text{cm}^3 \text{s}^{-1}$  for the *HF* and *DF* channels respectively, as compared with  $8.42 \times 10^{-12}$  and  $6.6 \times 10^{-12}$  on the SW-PES, and with  $7.2 \times 10^{-12}$  and  $5.66 \times 10^{-12}$  on the 6SEC one. As can be seen in Table 2, the QCT calculations on the older, collinear PESs like the M5 or the T5 lead to much lower rate constants [15].

The most complete experimental determination of the ratio of thermal rate constants for the two exit channels of *F+HD* was performed by Persky [2] in the temperature range between 159 and 413 K. The experiments were carried out in a discharge flow system with mass spectrometric analysis of the reaction products. A room temperature chemical laser measurement by Berry [3] was in very good agreement with the value of Persky. The data from the experiment of Persky, together with the present QCT results on the SW surface and those of Rosenman and Persky [15] on the 6SEC PES, are represented in the lower panel of Fig. 3. In the same figure (upper panel) the experimental intermolecular isotopic branching ratio of the thermal rate constants for *F+H<sub>2</sub>/F+D<sub>2</sub>* [26], as well as the corresponding QCT values obtained on the 6SEC [15] and SW [19] PES, are shown too. In the case of the SW surface, the intermolecular branching ratio reported in our previous work till  $T = 200 \text{ K}$  [19] is extended here to  $T = 150 \text{ K}$ . The divergence between experiment and theory with decreasing temperature is probably due to the neglect of tunneling inherent to the classical approach, which is expected to play an important role in the reactions leading to *HF*. In fact, the coupled states QM branching ratios reported recently by Rosenman et al. [20] on the SW-PES are in better agreement with the experimental data.

An inspection of the intramolecular branching ratio for the *F+HD* reaction (lower panel of Fig. 3) shows that over the whole temperature range considered, the *HF* exit channel is the preponderant one under thermal conditions. For the lowest temperature investigated, the experimental branching ratio is larger by about 25% than that from the present QCT calculations on the SW-PES. The experimental branching ratio decreases slightly with increasing temperature, whereas the theoretical one remains nearly constant.



For  $T \approx 400$  K, the difference between experiment and theory is close to 5%. The agreement with the analogous QCT results on the 6SEC-PES [15] is very good. It is interesting to observe that the temperature dependence of the intramolecular rate constant branching ratio obtained on the SW-PES is much weaker than that of the corresponding intermolecular one (upper panel). This finding is in qualitative agreement with the experimental results. In contrast, a weak dependence is obtained in both cases on the 6SEC-PES. The results on collinear PES are in worse agreement with the measurements yielding intramolecular branching ratios close to unity [15] in the whole temperature range. Although no QM calculations have been reported for this isotopic variant, the results commented on above suggest that tunneling should be more important for the *HF* exit channel and, thus, QCT results would be less reliable for this channel. A hint in this direction was found in the detailed analysis of the data from the molecular beam experiment of Neumark et al. [6] discussed in reference [13]. Therefore, it is likely that a contribution from tunneling favors the *HF* channel and, thus, the quantum mechanical *HF/DF* branching ratio should be higher than the classical one, especially for the lowest temperatures, in better agreement with the measurements.

In a later experiment, Johnston et al. [5] obtained the ratio of reaction cross sections for the two exit channels in the range between 4.5 and 8.3 kcal/mol (0.19-0.36 eV). The results of these measurements are represented in Fig. 4. In this experiment, carried out in a cell, excimer laser photolysis of  $F_2$  was used for the generation of the *F* atoms and vacuum ultraviolet laser induced fluorescence for the detection of the *H(D)* atomic products. Although the experiment was performed under single collision conditions, its dynamical resolution is not high due to the broad energy distributions implied. The comparison of these experimental branching ratios with the thermal ones discussed previously reflects a tendency towards a similar reaction probability for both ends with increasing collision energy. It should be noted however that the branching ratios of the experiments of Persky [2] and of Johnston et al. [5] are only approximately comparable since, in the latter experiment, the rotational states at  $\approx 300$  K are Boltzmann distributed, whereas the average collision energies are much higher than the thermal one at room temperature ( $E_T \approx 0.026$  eV). The simulation of the experimental conditions with QCT

data obtained on the SW-PES leads to *HF/HD* branching ratios in better accordance with the experimental data than calculations on the 6SEC PES, especially in the higher  $E_T$  range.

An inspection of the excitation functions of the present calculations (see Fig. 1) shows that the reactivity changes drastically with  $E_T$  for collision energies below 0.1 eV. Furthermore, in the *HF* reaction channel the excitation functions strongly increase with the rotational quantum number  $j$ . The cross sections pertaining to this region are precisely those corresponding to the experimental conditions, where the largest discrepancies between measurements and calculations are found. For collision energies larger than 0.2 eV the variations in the excitation functions with  $E_T$  are much smaller and, although for the *HF* channel the predicted influence of rotation on reactivity is still important, it should not have appreciable effects in experiments implying relatively broad rotational distributions. For the rotational distribution of the experiment of Johnston et al. [5] ( $T \approx 300$  K) the most populated rotational states of *HD* are  $j=2$ , 1 and 3 respectively and the QCT rotationally averaged cross sections for  $E_T > 0.2$  eV tend to be approximately  $4\text{\AA}^2$  for both channels, leading thus to a value of the branching ratio close to one, in accord with the experimental data.

#### 4. Conclusions

The available experimental data on rate constants and intramolecular branching ratios for the asymmetric *F+HD* reaction are, in general, well reproduced with QCT calculations on the present *ab initio* potential energy surface. Although some discrepancies persist in the low temperature region, these calculations provide the best global agreement obtained to date between experiment and theory for this reaction.

The essentials of the dynamics beneath the mentioned kinetic data are contained in the shapes of the rotationally state resolved excitation functions for the two exit channels, which in turn are determined both by the mass asymmetry of the molecule and by the precise features of the PES. In this respect it is important to emphasize that the extended

use of potential surfaces with collinear barriers and narrow bending potentials in theoretical calculations leads to too small rate constants and to a false consideration of the decisive beneficial influence of rotation on the *HF* exit channel, which is crucial for the interpretation of experimental data.

Further improvements of the PES, like the inclusion of spin-orbit coupling, the performance of accurate QM calculations and of experiments with higher resolution, especially in the low collision energy region, would certainly help to clarify the remaining discrepancies.

### **Acknowledgment**

The Spanish part of this work has been financed by the DGICYT under grant PB95-0918-CO2. The German part of this work received generous funding from the German Fonds der Chemischen Industrie. The Spanish-German exchange program Acciones Integradas is also acknowledged.

## References

- [1] K. L. Kompa, J. H. Parker and G. C. Pimentel, *J. Chem. Phys.* 49 (1968) 4257.
- [2] A. Persky, *J. Chem. Phys.* 59 (1973) 5578
- [3] M. J. Berry, *J. Chem. Phys.* 59 (1973) 6229.
- [4] K. Tsukiyama, B. Katz and R. Bersohn, *J. Chem. Phys.* 83 (1985) 2889
- [5] G. W. Johnston, H. Kornweitz, I. Schechter, A. Persky, B. Katz, R. Bersohn and R. D. Levine, *J. Chem. Phys.* 94 (1991) 2749
- [6] D. M. Neumark, A. M. Wodtke, G. N. Robinson, C.C. Hayden, R. Shobatake, R. K. Sparks, T. P. Schafer, and Y. T. Lee, *J. Chem. Phys.* 82 (1985) 3067.
- [7] J.-B. Song and E. A. Gislason, *J. Chem. Phys.* 104 (1996) 5834
- [8] J. T. Muckerman in *Theoretical Chemistry: Advances and Perspectives*, eds. H. Eyring and D. Henderson (Academic, New York, 1981).
- [9] T. Takayanagi and S. Sato, *Chem. Phys. Lett.* 144 (1988) 191
  
- [10] G. C. Lynch, R. Steckler, D. W. Schwenke, A. J. C. Varandas, D. G. Truhlar and B. C. Garrett, *J. Chem. Phys.* 94(1991) 7136
- [11] S. L. Mielke, G. C. Lynch, D. G. Truhlar and D. W. Schwenke, *Chem. Phys. Lett.* 213 (1993) 10
- [12] K. Stark and H.-J. Werner, *J. Chem. Phys.* 104 (1996) 6515
- [13] F. J. Aoiz, L. Bañares, V. J. Herrero, V. Sáez Rábanos, K. Stark and H.-J. Werner, *J. Chem. Phys.* 102 (1995) 9248.
- [14] J. F. Castillo, D. E. Manolopoulos, K. Stark and H.-J Werner, *J. Chem. Phys.* 104 (1996) 6531.
- [15] E. Rosenman and A. Persky, *Chem. Phys.* 195 (1995) 191
- [16] F. B. Brown, R. Steckler, D. W. Schwenke, D.G. Truhlar and B. C. Garrett, *J. Chem. Phys.* 82 (1985) 188..

- [17] R. Steckler, D. G. Truhlar and B. C. Garrett, *J. Chem. Phys.* 82 (1985) 5499
- [18] E. Rosenman, S. Hochman-Kowal, A. Persky and M. Baer, *J. Phys. Chem.* 99 (1995) 16523.
- [19] F. J. Aoiz, L. Bañares, V. J. Herrero, K. Stark and H.-J. Werner, *Chem. Phys. Lett.* 254 (1996) 341.
- [20] E. Rosenman, S. Hochman-Kowal, A. Persky and M. Baer, *Chem. Phys. Lett.* 257 (1996) 421.
- [21] F. J. Aoiz, L. Bañares, T. Diez-Rojo, V. J. Herrero and V. Sáez-Rábanos, *J. Phys. Chem.* 100 (1994) 4071.
- [22] V. M. Azriel, G. D. Billing, L. Yu. Rusin and M. B. Sevryuk *Chem. Phys.* 195 (1995) 243.
- [23] J.-B. Song and E. A. Gislason, *J. Chem. Phys.* 99 (1993) 5117
- [24] F. J. Aoiz, L. Bañares, V. J. Herrero and V. Sáez Rábanos, *Chem. Phys.* 187 (1994) 227.
- [25] N. Cohen and K. R. Westberg, *J. Phys Chem. Ref. Data.* 12 (1983) 531
- [26] A. Persky, *J. Chem. Phys.* 59 (1973) 3612

## FIGURE CAPTIONS

Fig. 1. Total QCT reaction cross sections as a function of collision energy (excitation function) calculated on the SW-PES for the reaction of fluorine atoms with  $HD$  molecules in selected rotational states. Upper panel,  $HF+D$  exit channel; lower panel,  $DF+H$  exit channel. The error bars correspond to one standard deviation.

Fig. 2. Comparison of thermal rate constants for the  $F+HD$  reaction calculated on two different PES. Upper panel, rate constants for the production of  $HF+D$ ; lower panel, rate constants for the production of  $DF+H$ . The circles with error bars connected by a solid line are the results of the present QCT calculation on the SW-PES; the squares connected by a dashed line correspond to the QCT calculations of Rosenman and Persky [15] on the 6SEC-PES.

Fig. 3. Comparison of intermolecular ( $k_{F+H2}/k_{F+D2}$ )-and intramolecular ( $k_{F+HD}/k_{F+DH}$ ) kinetic isotope branching ratio (upper and lower panel respectively) from experiment and theory. Squares: measurements of Persky [2,26] dashed line QCT calculation of Rosenman and Persky [15] on the 6SEC PES, solid lines: present QCT calculation on the SW-PES.

Fig. 4 Comparison of the experimental and theoretical intramolecular isotopic branching ratio  $\sigma_R(HF+D)/\sigma_R(DF+H)$  of the reaction cross sections as a function of collision energy. Solid circles with boxes: Experiment of Johnston et al. [5], the boxes account for the error in the determination of the branching ratio and the uncertainty in the collision energy; circles with a solid line: present QCT calculations on the SW-PES; squares with a dashed line: QCT calculations of Rosenman and Persky [15] on the 6SEC-PES.

Table 1: Specific rate constants  $k(T, j)$  ( $\text{cm}^3 \text{s}^{-1}$ ) for the  $\text{F}+\text{HD}(v=0, j=0-6) \rightarrow \text{HF}(\text{DF})+\text{D}(\text{H})$  reaction as a function of temperature calculated on the SW PES. Numbers in parentheses represent powers of ten.

HF+D channel				
T(K)	$j = 0$	$j = 1$	$j = 2$	$j = 3$
200	$2.32 \pm 0.14(-12)$	$5.62 \pm 0.26(-12)$	$1.27 \pm 0.04(-11)$	$1.66 \pm 0.04(-11)$
250	$4.28 \pm 0.21(-12)$	$9.46 \pm 0.33(-12)$	$1.90 \pm 0.04(-11)$	$2.44 \pm 0.05(-11)$
300	$6.55 \pm 0.26(-12)$	$1.37 \pm 0.04(-11)$	$2.54 \pm 0.05(-11)$	$3.22 \pm 0.05(-11)$
350	$9.02 \pm 0.30(-12)$	$1.81 \pm 0.04(-11)$	$3.16 \pm 0.05(-11)$	$3.98 \pm 0.06(-11)$
400	$1.16 \pm 0.03(-11)$	$2.26 \pm 0.04(-11)$	$3.76 \pm 0.05(-11)$	$4.70 \pm 0.06(-11)$
450	$1.43 \pm 0.03(-11)$	$2.71 \pm 0.04(-11)$	$4.34 \pm 0.05(-11)$	$5.39 \pm 0.06(-11)$
500	$1.70 \pm 0.04(-11)$	$3.14 \pm 0.05(-11)$	$4.89 \pm 0.05(-11)$	$6.04 \pm 0.06(-11)$
T(K)	$j = 4$	$j = 5$	$j = 6$	
200	$2.09 \pm 0.04(-11)$	$2.12 \pm 0.04(-11)$	$2.54 \pm 0.05(-11)$	
250	$3.06 \pm 0.05(-11)$	$3.13 \pm 0.05(-11)$	$3.65 \pm 0.06(-11)$	
300	$4.00 \pm 0.06(-11)$	$4.12 \pm 0.05(-11)$	$4.74 \pm 0.06(-11)$	
350	$4.90 \pm 0.06(-11)$	$5.09 \pm 0.06(-11)$	$5.78 \pm 0.06(-11)$	
400	$5.75 \pm 0.06(-11)$	$6.00 \pm 0.06(-11)$	$6.75 \pm 0.06(-11)$	
450	$6.54 \pm 0.06(-11)$	$6.86 \pm 0.06(-11)$	$7.66 \pm 0.07(-11)$	
500	$7.28 \pm 0.06(-11)$	$7.67 \pm 0.06(-11)$	$8.52 \pm 0.07(-11)$	
DF+H channel				
T(K)	$j = 0$	$j = 1$	$j = 2$	$j = 3$
200	$4.66 \pm 0.16(-12)$	$5.67 \pm 0.23(-12)$	$5.19 \pm 0.30(-12)$	$5.07 \pm 0.31(-12)$
250	$9.02 \pm 0.23(-12)$	$1.01 \pm 0.03(-11)$	$9.08 \pm 0.37(-12)$	$8.80 \pm 0.39(-12)$
300	$1.43 \pm 0.03(-11)$	$1.52 \pm 0.04(-11)$	$1.36 \pm 0.04(-11)$	$1.31 \pm 0.04(-11)$
350	$2.01 \pm 0.03(-11)$	$2.07 \pm 0.04(-11)$	$1.86 \pm 0.05(-11)$	$1.78 \pm 0.05(-11)$
400	$2.62 \pm 0.04(-11)$	$2.64 \pm 0.04(-11)$	$2.38 \pm 0.05(-11)$	$2.28 \pm 0.05(-11)$
450	$3.23 \pm 0.04(-11)$	$3.21 \pm 0.05(-11)$	$2.91 \pm 0.05(-11)$	$2.78 \pm 0.05(-11)$
500	$3.85 \pm 0.04(-11)$	$3.78 \pm 0.05(-11)$	$3.44 \pm 0.05(-11)$	$3.29 \pm 0.05(-11)$
T(K)	$j = 4$	$j = 5$	$j = 6$	
200	$6.11 \pm 0.35(-12)$	$8.65 \pm 0.39(-12)$	$1.09 \pm 0.04(-11)$	
250	$9.72 \pm 0.41(-12)$	$1.29 \pm 0.04(-11)$	$1.58 \pm 0.05(-11)$	
300	$1.37 \pm 0.04(-11)$	$1.74 \pm 0.05(-11)$	$2.07 \pm 0.05(-11)$	
350	$1.79 \pm 0.05(-11)$	$2.20 \pm 0.05(-11)$	$2.56 \pm 0.05(-11)$	
400	$2.24 \pm 0.05(-11)$	$2.65 \pm 0.05(-11)$	$3.05 \pm 0.05(-11)$	
450	$2.69 \pm 0.05(-11)$	$3.10 \pm 0.05(-11)$	$3.52 \pm 0.05(-11)$	
500	$3.14 \pm 0.05(-11)$	$3.55 \pm 0.05(-11)$	$3.98 \pm 0.05(-11)$	

Table 2: Thermal rate constants  $k(T)$  ( $\text{cm}^3 \text{ s}^{-1}$ ) for the  $\text{F}+\text{HD}\rightarrow\text{HF}(\text{DF})+\text{D}(\text{H})$  reaction as a function of temperature calculated on the SW PES and taking into account the multisurface factor (see text). Numbers in parentheses represent powers of ten.

HF+D channel				
T(K)	SW PES	6SEC PES <sup>†</sup>	T5A PES <sup>†</sup>	M5 PES <sup>†</sup>
159	1.61±0.17(-12)	1.17(-12)	9.60(-13)	5.00(-13)
168	1.93±0.19(-12)	1.43(-12)	1.13(-12)	6.00(-13)
200	3.27±0.26(-12)			
222	4.32±0.30(-12)	3.48(-12)	2.27(-12)	1.35(-12)
250	5.77±0.34(-12)			
298	8.42±0.40(-12)	7.20(-12)	3.95(-12)	2.54(-12)
300	8.53±0.40(-12)			
350	1.14±0.04(-11)			
400	1.42±0.05(-11)			
413	1.49±0.05(-11)	1.32(-11)	6.20(-12)	4.23(-12)
450	1.70±0.05(-11)			
500	1.96±0.05(-11)			
DF+H channel				
T(K)	SW PES	6SEC PES <sup>†</sup>	T5A PES <sup>†</sup>	M5 PES <sup>†</sup>
159	1.25±0.14(-12)	8.60(-13)	9.20(-13)	4.60(-13)
168	1.50±0.16(-12)	1.06(-12)	1.08(-12)	5.60(-13)
200	2.56±0.23(-12)			
222	3.39±0.27(-12)	2.66(-12)	2.17(-12)	1.32(-12)
250	4.52±0.31(-12)			
298	6.60±0.38(-12)	5.66(-12)	3.76(-12)	2.61(-12)
300	6.69±0.38(-12)			
350	8.91±0.42(-12)			
400	1.11±0.05(-11)			
413	1.17±0.05(-11)	1.06(-11)	5.89(-12)	4.50(-12)
450	1.32±0.05(-11)			
500	1.53±0.05(-11)			

<sup>†</sup> Ref. [15]



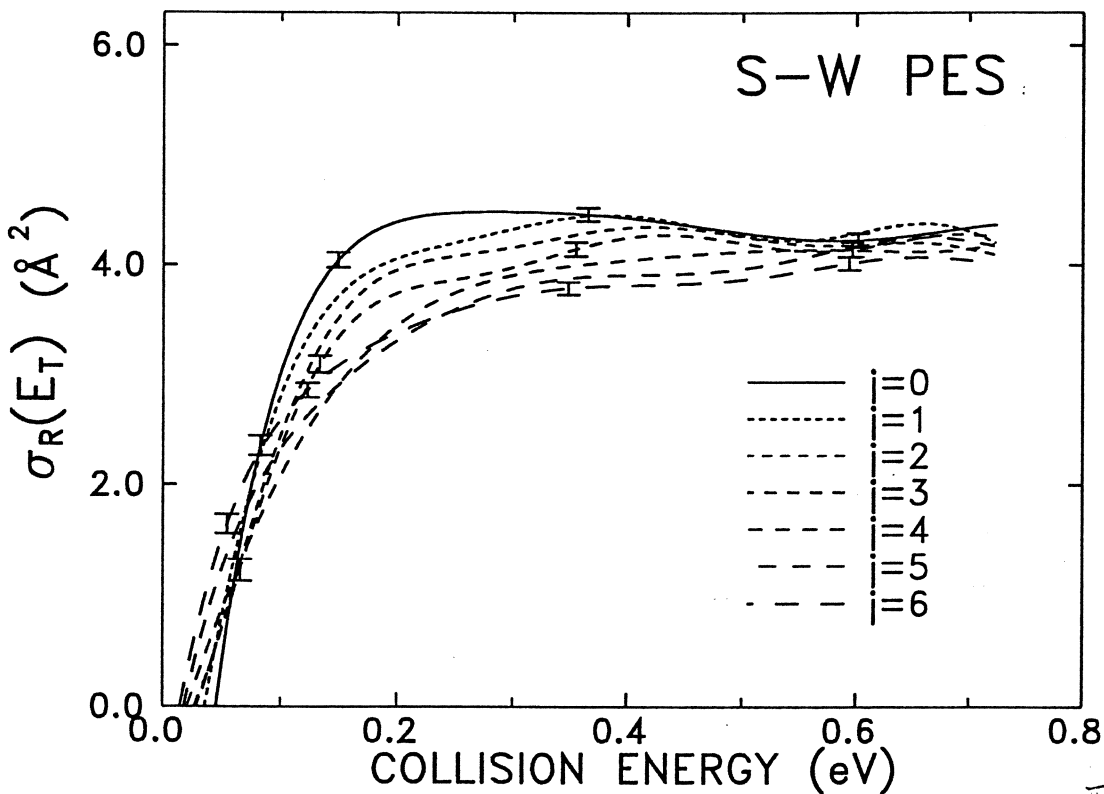
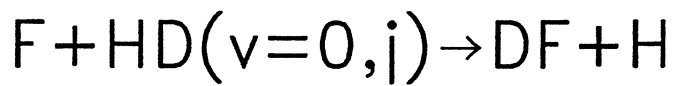
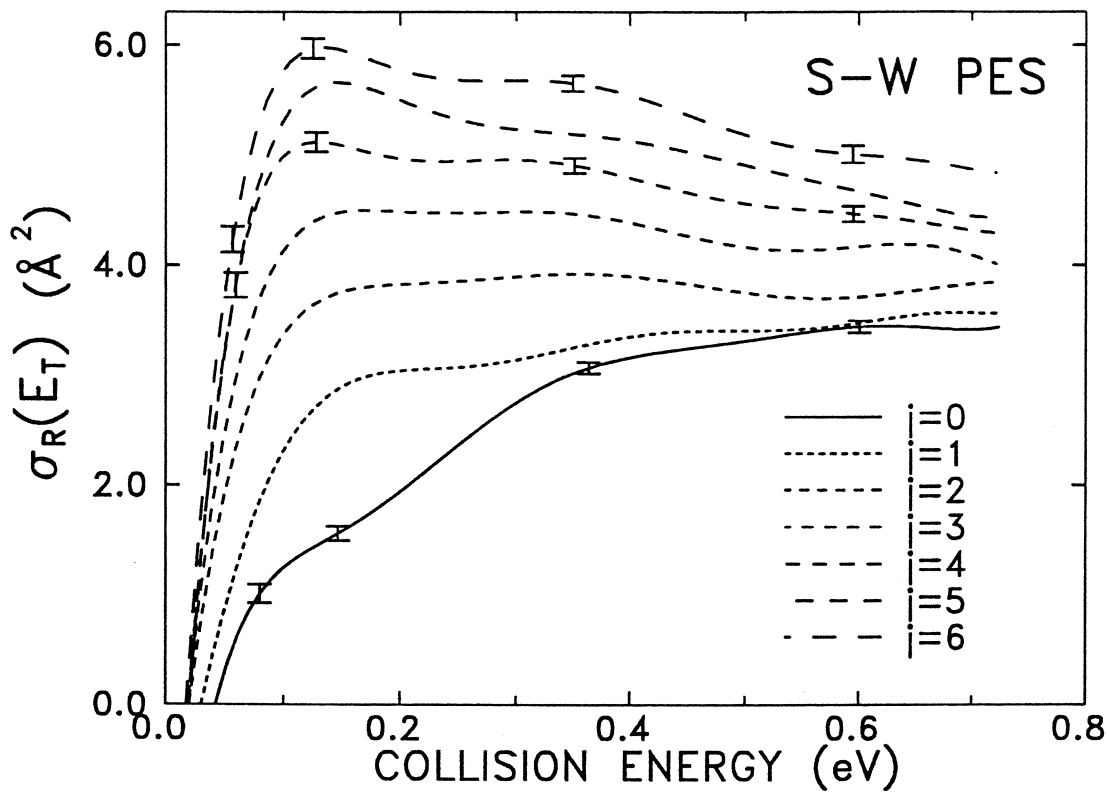
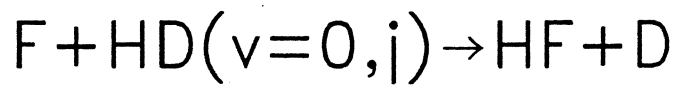


Fig 1.  
Aoi et al.

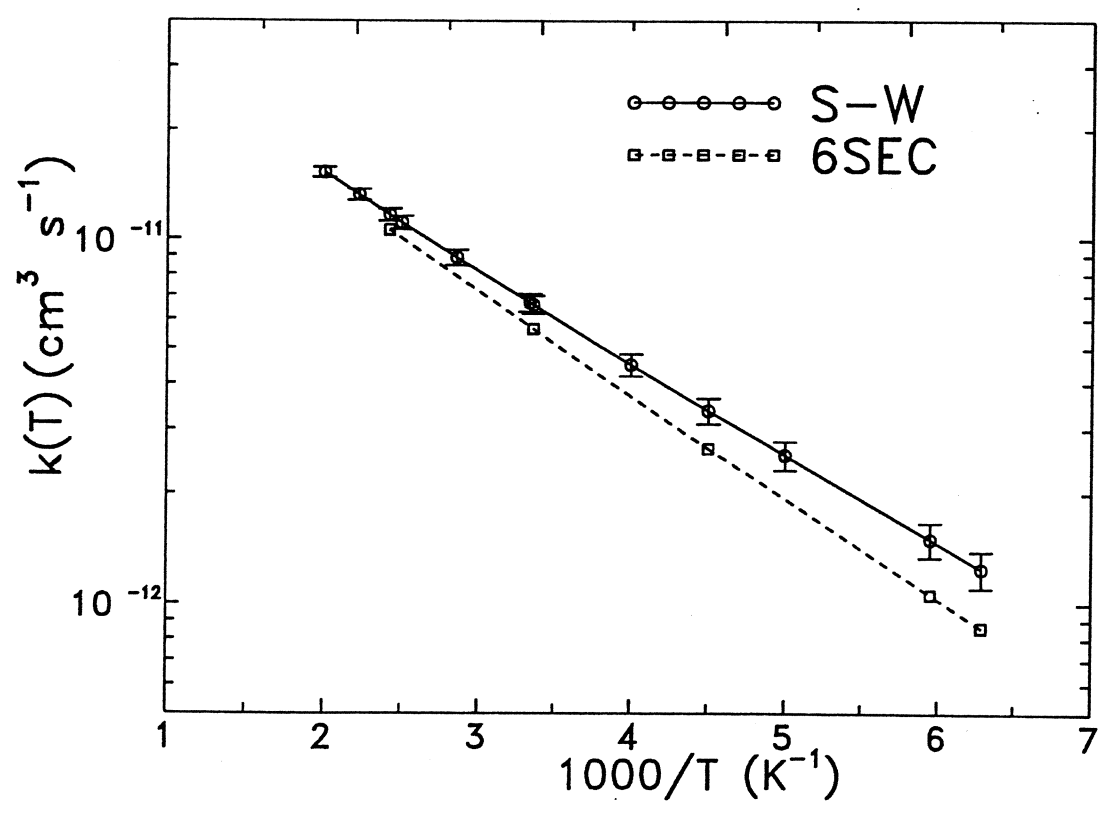
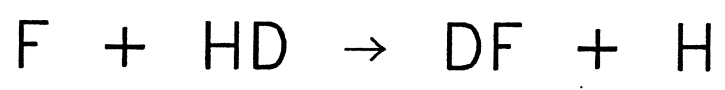
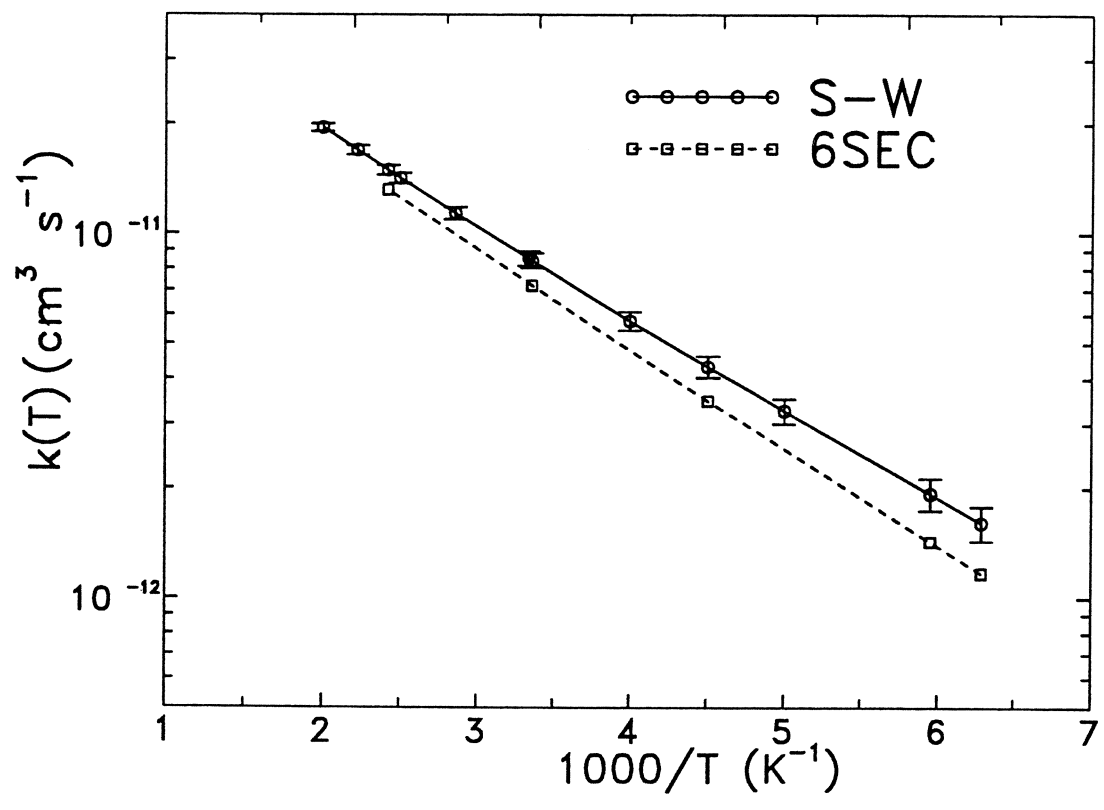
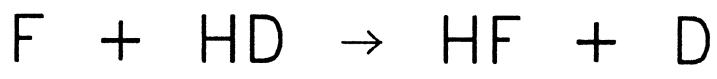
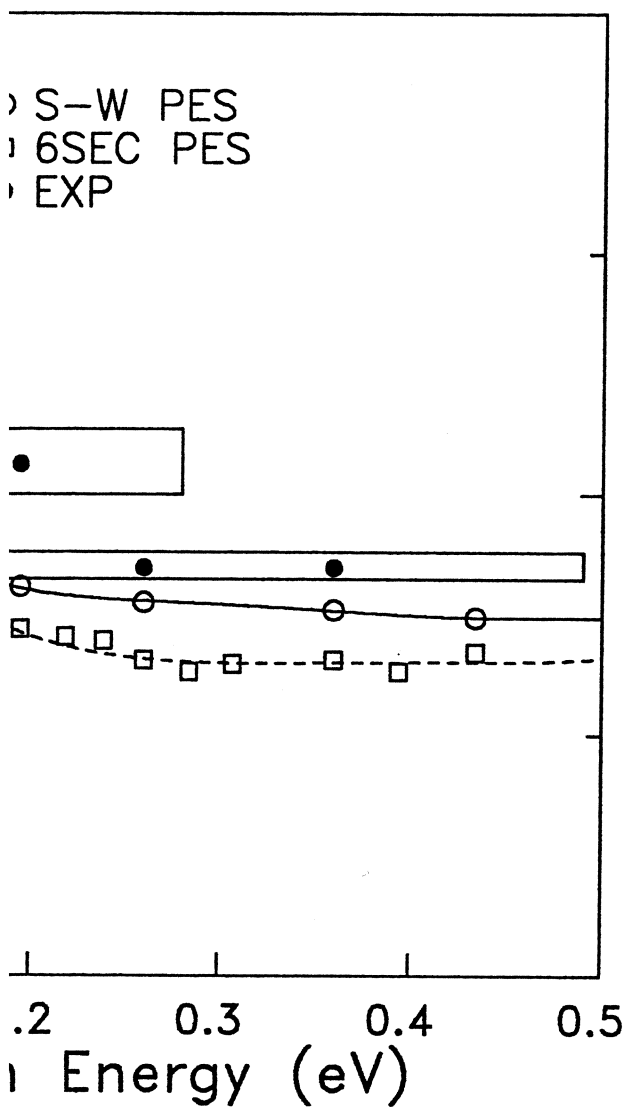
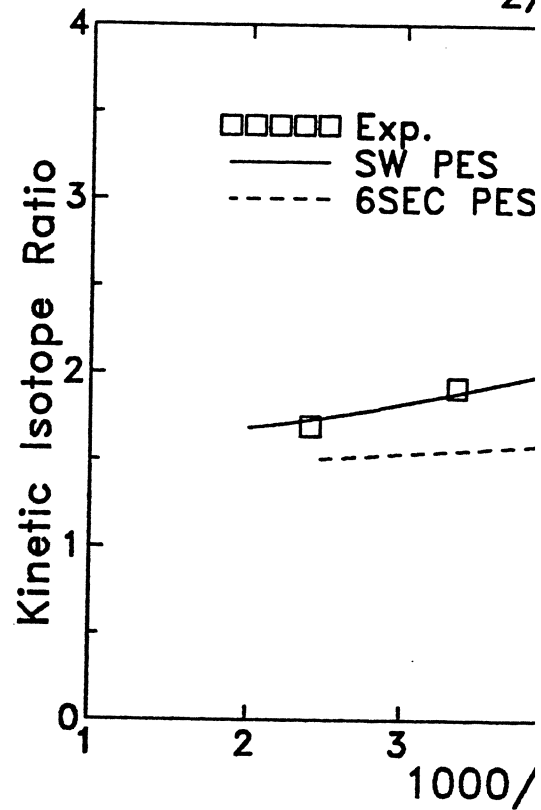


Fig. 2  
Aoi et al.

$F+D/DF+H$



$F+n-H_2$



$F+HD$

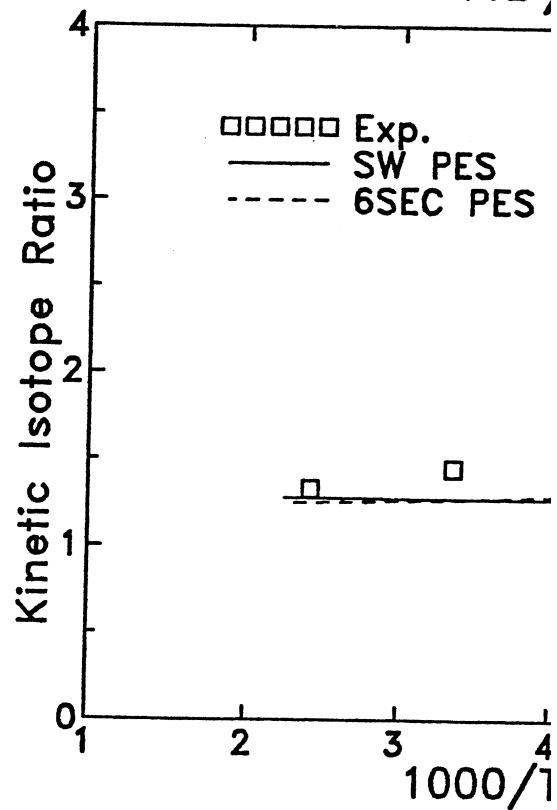


Fig. 4.  
Aoi et al.